scientific reports

Check for updates

OPEN

Plasmonic optical fiber biosensors for ultra-low detection of respiratory syncytial virus via point-of-care tests

Federica Passeggio[1,2], Luigi Zeni[1], Massimiliano Galdiero[3,4], Francesco Arcadio[1], Carla Zannella[3], Anna De Filippis[3], Chiara Marzano[1], Ines Tavoletta[1], Fabiana Napolitano[2], Rosalba Pitruzzella[1], Giuseppe Portella[2]✉ & Nunzio Cennamo[1]✉

Respiratory syncytial virus (RSV) is a major cause of bronchiolitis and pneumonia, particularly in children, the elderly, and immunocompromised individuals. Despite significant health impacts, annual RSV-related hospitalizations may be underreported due to undertesting and limited diagnostic sensitivity. Point-of-care tests (POCTs) could enhance the rapid and accurate detection of RSV, enabling timely treatment and reducing hospitalizations. In this frame, for the first time, a plasmonic RSV biosensor based on modified plastic optical fibers (POFs) has been developed and tested by functionalizing the plasmonic platform with a specific antibody targeting the RSV fusion (F) protein. This protein was selected because it is the most conserved surface protein between the two RSV subtypes, RSV A and RSV B. The main goal of the work is to develop a biosensor capable of detecting RSV regardless of the subtype (A or B), as subtype discrimination is not clinically relevant for therapeutic decision-making. The POF-based RSV biosensor performance was first obtained via standard solutions with different RSV concentrations to evaluate the binding sensitivity with the target analyte. In such a way, an ultra-low detection limit equal to about 0.88 PFU/mL was achieved. Furthermore, selectivity tests demonstrated the biosensor's ability to distinguish RSV from other viruses. In addition, nasopharyngeal swab samples were tested. The POCT's RSV measurement time is about ten minutes. A gold standard analysis confirmed the achieved results. Hence, the results establish the POF-based RSV biosensor as a sensitive, cost-effective, ultra-fast, capable of being connected to the Internet, and a scalable alternative to traditional RSV detection methods, offering a promising tool for improving diagnostic capabilities in clinical and resource-limited settings.

RSV is a non-segmented RNA virus, with negative polarity, belonging to the Paramyxoviridae family and the Pneumonvirinae subfamily. The virion is characterized by a round shape with a diameter of 80–500 nm or a filamentous one of 5000 nm[1]. It has a lipid coating (envelope) enclosing a helically symmetric nucleocapsid. The 15.2 kb RSV genome encodes 10 genes that are translated into 11 viral proteins [2]. Two RSV antigenic subtypes are known RSV-A and RSV-B. Glycoproteins G and F, responsible for viral attachment and fusion, are major antigenic targets for neutralizing antibodies [2]. G protein is responsible for the adhesion of the virus to the receptors of the host cell, while the F protein induces the fusion of the viral envelope with the host cell surface. F protein plays a role in pathogenesis, inducing the formation of syncytia and multinucleated giant cells leading to cell death[3].

Among RSV proteins, the G-protein exhibits the most variability, with two hypervariable regions that contribute to antigenic differences both between and within RSV subtypes. In contrast, the F-protein is highly conserved across both subtypes and serves as a target for vaccines and monoclonal antibodies. The F (fusion) protein of RSV is particularly well-conserved between the two major subtypes, A and B, sharing approximately 89% amino acid sequence identity. On the other hand, the G-protein shows much less conservation, with only

[1]Department of Engineering, University of Campania "Luigi Vanvitelli", Aversa 81031, Italy. [2]Department of Translational Medical Sciences, University of Naples "Federico II", Naples 80131, Italy. [3]Department of Experimental Medicine, Section of Microbiology and Clinical Microbiology, University of Campania "Luigi Vanvitelli", Naples 80138, Italy. [4]Complex Operative Unit of Virology and Microbiology, University Hospital of Campania "Luigi Vanvitelli", Naples 80138, Italy. ✉email: giuseppe.portella@unina.it; nunzio.cennamo@unicampania.it

about 53% sequence similarity. The differences in the F-protein between subtypes A and B are limited to just 25 amino acids, making it an ideal target for diagnostic tools, monoclonal antibodies, and vaccine development[4].

RSV is the most common viral cause of serious respiratory illness in children under the age of five, as well as the major cause of pediatric bronchiolitis [5]. RSV-associated acute lower respiratory infections are estimated to result in approximately 3.6 million hospitalizations and 26,300 deaths annually among children aged 0–60 months[6]. Since most of these deaths occur in developing countries, it is likely an underestimation of these figures. RSV does not only affect children: old and immunocompromised subjects are also severely affected. In USA an estimated 100,000–160,000 adults over 60 years old are hospitalized following RSV infection. The highest risk for severe RSV disease includes older adults (>75 years) or subjects with chronic heart or lung diseases, immunocompromised, or with other underlying medical conditions, including diabetes or obesity. After infection with a single strain of RSV, only partial immunity can be achieved at most, hence re-infections could happen throughout life.

A protein-based maternal vaccine is available to protect newborns within 90 days from birth, a monoclonal antibody (mAb) is now -approved for passive immunisation of the infants, whereas an mRNA and two protein-based vaccines are approved for older adults.

From October 2024, vaccine is recommended for all newborns during the first season of exposure to RSV. Vaccination of infants in high-income countries has already shown positive public health results, and protection is expected globally in the coming years[7]. While RSV immunization is now available in income countries, global access is not accomplished yet, and worldwide prevention is not within reach.

RSV infection is a frequent cause hospitalization of infants, children, and the elderly. The seasonality of this virus and non-specific clinical manifestations overlaps with other viral and bacterial agents making difficult to discriminate between viral and bacterial infections resulting in overprescription of antibiotics [8].

Since a clinical diagnosis is not easily achieved, efficient, cheap and rapid assays for the detection of RSV are required. Currently, the gold standard for RSV detection is the Real Time-PCR testing, with an excellent sensitivity and specificity (close to 99%). However, RT PCR testing has several limitations including costs, the need for complex instrumentation and qualified staff[8].

Rapid multiplex PCR tests are also available, searching for RSV, Influenza A and B and other viruses. These assays are easy to perform and do not require a qualified staff or instruments. However, few samples can be analysed at the same time and require 30 min–1 h depending on the manufacturer. In addition, the sensitivity of these rapid PCR assays is not the same of traditional RT-PCR assays.

Antigenic point-of-care tests (POCTs) for RSV detection could allow early detection in the emergency department, avoiding sending samples to the lab. Subsequently, a specific and effective therapy can be immediately established, reducing the number and duration of hospitalizations[8–10]. POCTs are easy to perform and provide results in a few minutes. However, only moderate sensitivity for RSV has been reported, therefore the clinical use of the tests needs to be carefully assessed[12]. Moreover, the sensitivity of these assays is lower than RT-PCR, especially when the Ct values are more than 30, making necessary to confirm negative results by RT-PCR, at least in patients with severe symptoms[13]. In most cases, antigenic tests could result ineffective because 10–30% of patients with respiratory virus infections continue to be serologically negative. In addition, serological assays also do not provide reliable results during the off-season[14].

Biosensors could represent a suitable solution for the rapid detection of viruses and bacteria, offering high sensitivity, specificity, and quick response times. Compared to traditional laboratory methods, these devices enable more immediate and low-cost identification of pathogens, which is critical in public health emergencies and environmental monitoring.

More specifically, the integration of biosensors with plastic optical fibers (POFs) opens to new possibilities for real-time detection of viruses and bacteria as well to monitor the disease and the therapy. POF-based biosensors are particularly suited for developing POCTs due to their flexibility, robustness, and cost-effectiveness, making them ideal for use in harsh environments and remote sensing[15]. POFs can be combined with molecular recognition elements (MREs), which can be either biological (e.g., antibodies, aptamers, etc.) or synthetic (as in the case of molecularly imprinted polymers (MIPs))[15–17]. Among other sensing techniques, transducer based on surface plasmon resonance (SPR), which is an extremely sensitive phenomenon to refractive index (RI) variations at the interface between a dielectric medium and a nanometric metal film, and combined with specific receptors, allows molecular interactions to be monitored in real-time. In this regard, several works have been proposed in the literature that exploit plasmonic sensors for the detection of viruses and bacteria[15,18,19].

A SARS-CoV-2 sensor was developed by exploiting an SPR-POF probe coupled with an MIP nano-layer, specifically designed for the recognition of Subunit 1 of the SARS-CoV-2 spike protein. Preliminary results relative to SARS-CoV-2 virion detection performed on nasopharyngeal (NP) swabs were compared to those obtained with RT-PCR, demonstrating that the proposed optical-chemical sensor had higher sensitivity than the gold standard technique[20]. Furthermore, SARS-CoV-2 spike protein was monitored via the same SPR-POF probe combined with an aptamer layer specifically obtained using the receptor-binding domain (RBD) of the SARS-CoV-2 spike protein[21]. After a preliminary characterization to monitor the protein detection, tests on the SARS-CoV-2 positive sample in universal transport medium (UTM) 1:2 diluted were performed, encouraging its application as a POCT device[21].

Along the same line, an SPR-POF biosensor for the *Brucella abortus* bacterium detection was recently presented[22]. In particular, the SPR sensitive surface was functionalized with a bio-receptor layer specific for the bacterium membrane protein[22].

In this study, a plasmonic POF-based biosensor was developed for the selective detection of RSV. To obtain the RSV biosensor chip, the SPR-POF probe was functionalized with a specific antibody for the F protein of the RSV. The choice to functionalize with an antibody to a membrane protein (F protein) allows for direct detection of the virus within clinical samples, without the need for pre-treatment. The proposed RSV biosensor can detect

RSV regardless of the subtype (A or B), as subtype discrimination is not clinically relevant for therapeutic decision-making. Therefore, it was essential to select a biomarker that is highly conserved across both subtypes to ensure broad applicability and consistent diagnostic performance.

First, the RSV biosensor was tested with solutions at different concentrations of virus in phosphate buffer, in order to evaluate the biosensing parameters, particularly limit of detection and sensitivity at low concentrations. Then, the biosensor's selectivity was evaluated by testing it in the presence of potential interfering viruses (i.e., human coronavirus and flu virus). Finally, the biosensor chip was tested in a real scenario using nasopharyngeal swab samples in UTM. The results were compared with those obtained with the RT-PCR technique, as a gold standard approach, highlighting the potential of the proposed POF-based RSV biosensor in POCT.

Materials and methods

Chemicals

N-Hydroxysuccinimide (NHS), N-(3-Dimethylaminopropyl)-N′-ethylcarbodiimide hydrochloride (EDC), (±)-α-Lipoic acid, ethanolamine, phosphate buffered saline (PBS) were purchased from Merck KGaA (Darmstadt, Germany); Anti-Respiratory Syncytial Virus antibody [2F7] was purchased from ABCAM (Cambridge, CB2 0AX, UK).

SPR-POF probe

The SPR-POF probe used to detect RSV was developed as thoroughly described in [23]. Briefly, the conventional plasmonic sensor is based on a modified POF, where a portion of the core is exposed creating a planar D-shaped POF surface that is then covered by an optical buffer layer (Microposit S1813 photoresist). This layer (about 1 µm thick) has a high RI (1.61 RIU) so to improve the plasmonic performance of the sensor and, moreover, it improves the adhesion with the subsequent nanometric metal layer [23]. In fact, to excite the SPR phenomenon, a gold nanofilm (60 nm thick) is deposited by a sputter coater machine (Safematic CCU-010, Zizers, Switzerland) on the buffer layer. Figure 1a shows the schematic cross-section of the SPR-POF probe during the production steps (step by step), whereas Figure S1 in Supplementary Information File summarizes all the details in terms of size via a cross-section outline of the probe.

Functionalization process of the SPR-POF probe

To develop the SPR-POF biosensor specific for the detection of RSV, a self-assembled monolayer (SAM) was fabricated onto the plasmonic probe sensitive surface by using an antibody targeting the RSV fusion protein as the bioreceptor. The functionalization of the plasmonic D-shaped POF consisted of various steps, following previously reported processes[24,25], as outlined in Fig. 1b. In particular, the sensitive surface was cleaned with Milli-Q water (3 times, 5 min each) and then treated with lipoic acid for 18 h (0.3 mM in 8% ethanol solution) to expose carboxyl groups; next, the surface was activated with NHS/EDC mixture (200 mM/50 mM in PBS, pH 7.4) for 20 min and washed three times with PBS. Then, the sensitive surface was incubated 2 h with about 10 µL of antibody (concentration of 0.5 mg/mL) for covalent immobilization. Successively, ethanolamine (1 M, pH 8.0) was used for 30 min to block the remaining free activated carboxyl groups. Finally, the functionalized platforms were stored in PBS overnight at 4 °C before use.

Experimental setup

The experimental setup used to test the SPR-POF biosensor consists of a white light source (model HL–2000–LL, manufactured by Ocean Optics, Orlando, FL, USA) with an emission range from 360 nm to 1700 nm and a spectrometer (model SR-6VN500, manufactured by Ocean Optics, Orlando, FL, USA) with a detection range of approximately 300 nm to 1000 nm. The SPR-POF biosensor is connected to the light source and the spectrometer

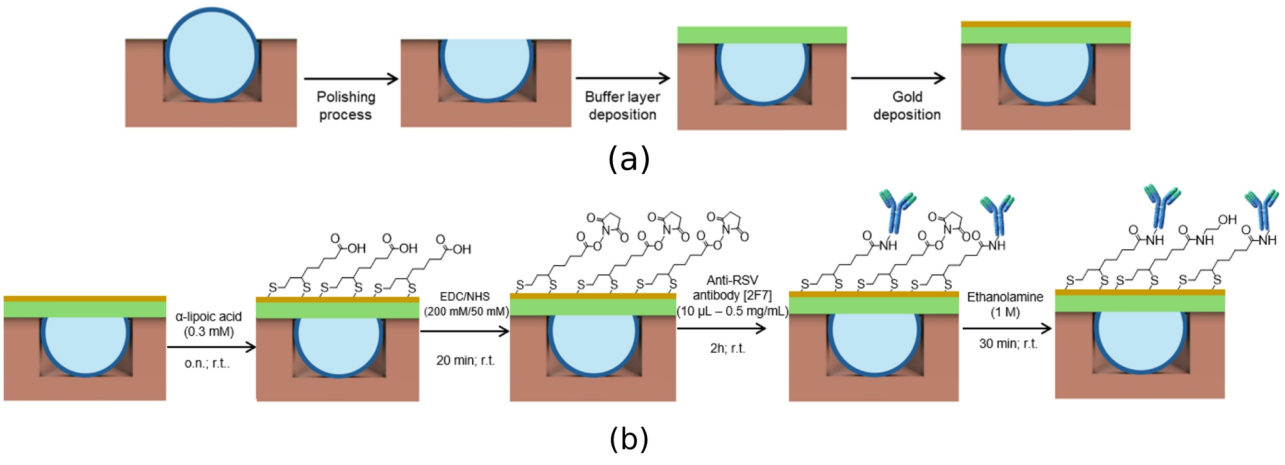

Fig. 1. Cross-section outline: (**a**) Production steps to make SPR-POF probes; (**b**) Functionalization process of the SPR-POF probes to achieve the RSV biosensors.

via removable SMA connectors. The spectrometer is then connected to a laptop, where the raw data are acquired via proprietary software (OceanView, version 2.0.16, Ocean Optics, Orlando, FL, USA) and then processed by Matlab software (version R2022b, Mathworks, Natick, MA, USA).

Figure 2 shows an actual image of the sensor chip (a) and of the experimental setup (b) used to carry out all the measurements.

Cells and viruses culture

Vero (ATCC CCL-81, Manassas, VA, USA) and Madin-Darby canine kidney (MDCK) cells (ATCC CCL-34) were cultured in Dulbecco's Modified Eagle Medium (DMEM) with 4.5 g/L glucose (Microtech, Naples, Italy), supplemented with penicillin/streptomycin solution (Himedia, Naples, Italy) and 10% fetal bovine serum (FBS) (Microtech). Vero cells were infected with RSV strain A2 (ATCC VR-1540) and human coronavirus 229E (HCoV-229E, ATCC VR-740) at the multiplicity of infection (MOI) of 0.1; MDCK were used to propagate influenza virus (flu-A, H1N1 STRAIN A/PR/8/34, ATCC VR-95) at MOI of 0.1 as before. When the cytopathic

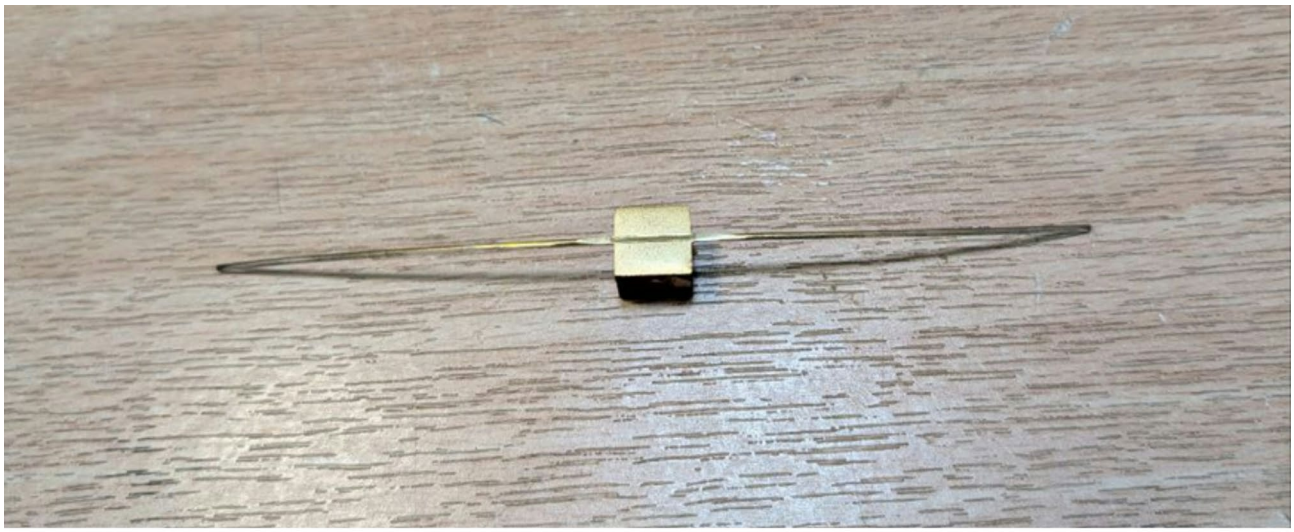

(a)

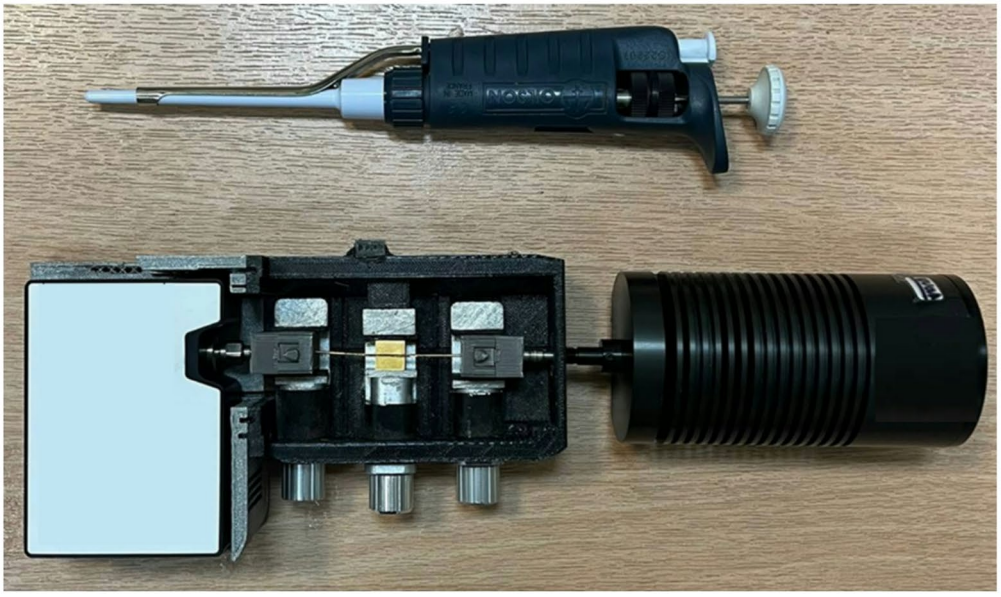

(b)

Fig. 2. (**a**) Picture of the POF biosensor chip. The sensitive area on the SPR-POF chip is 1 cm in length and 1 mm wide. (**b**) Picture of the small-sized experimental setup used for all measurements based on a light source, SPR-POF biosensor chip, and a spectrometer.

effect (CPE) was observed, cells were harvested and the viral titer was determined via plaque-assay. The original stock titer (PFU/mL) of RSV and HCoV-229E was 10^8 plaque-forming unit (PFU)/mL, and for flu-A was 10^6 PFU/mL.

qPCR

On the day of infection, serial 10-fold dilutions (from 1 PFU/mL to 10^5 PFU/mL) of RSV stock (propagated as discussed above) were prepared and used to infect a confluent monolayer of Vero cells. Viral RNA was extracted by TRIzol (Thermo Fisher Scientific, Waltham, MA, United States) from the RSV culture, when the CPE was observed, and quantified by evaluating the absorbance at Nanodrop (NanoDrop 2000, Thermo Fisher Scientific). The 5× All-In-One RT MasterMix (Applied Biological Materials, Richmond, Canada) was used to retrotranscribe RNA to cDNA; then, different dilutions of cDNA were prepared and 2 µL of each were amplified by a quantitative polymerase chain reaction (qPCR). The expression of gene coding for RSV F protein (forward sequence: TGCTCTGAGAACTGGTTGGT; reverse sequence: TTGTTGCTGGTGTGCTTTGC) was analyzed. Relative target threshold cycle (Ct) values were normalized to Glyceraldehyde 3-phosphate dehydrogenase (GAPDH; forward sequence: CCTTTCATTGAGCTCCAT; reverse sequence: CGTACATGGGAGCGTC), used as housekeeping gene. Primers were designed on Primer3 software (version 4.1.0)[26] and acquired from Eurofins (Ebersberg, Germany).

Western blot

Vero (1×10^6 cells) were infected with RSV at 0.1 MOI. And collected at different hours post-infection (hpi): then RIPA buffer (50 mM Tris-HCl, pH = 7.4; 150 mM NaCl; 0.5 M EDTA, 1% NP-40; 0.5% sodium deoxycholate; 0.1% SDS; phosphatase and protease inhibitors 1X) was used for protein extracts (30 µg) subjected to SDS-PAGE as reported elsewhere[27,28]. After the run, transfer to PVDF membranes (Millipore Corporation, Darmstadt, Germany) and blocking with 5% BSA, filters were incubated with the following antibodies: anti-RSV antibody [2F7] (Mouse Monoclonal Respiratory Syncytial Virus antibody, 1:1000, ab43812, ABCAM), anti-α-GAPDH (E-AB-48016, 1:10000, Elabscience, Houston, Texas, USA), and the horseradish peroxidase conjugated goat anti-mouse IgG (Biorad, Berkeley, CA, USA). Finally, detection was carried out by an enhanced chemiluminescence (ECL) (Thermo Scientific, Rockford, IL, USA) via ChemiDoc Imaging System (Bio-Rad, Hercules, California, United States). Immunoreactive bands were quantified by ImageLab 6.1 software (Bethesda, MD, USA).

Samples Preparation and measurement protocol for SPR-POF biosensors

The proposed biosensor chip using the F protein as the target allows for the direct detection of the virus in the sample without requiring a preliminary lysis step, which would otherwise be required if targeting the nucleoprotein. This additional step would make the procedure more complex and increase the turnaround time, thereby reducing the efficiency of our approach in a rapid diagnostic setting. As part of our protocol, only a single dilution step is performed before the sample is introduced to the biosensor. This simple operation is included to minimize potential matrix effects, which could otherwise result in non-specific binding with the sensitive surface. As previously mentioned, the F protein is essential for viral entry into host cells, a role that imposes strong evolutionary constraints and limits its potential for significant mutations. This high level of conservation makes it a stable and reliable target for diagnostic applications. Consequently, the choice of the F protein aligns with our goal of developing a rapid, straightforward, and user-friendly test, while ensuring high diagnostic sensitivity and specificity.

Virus samples were prepared from the stock (RSV concentration of approximately 10^8 PFU/mL in DMEM) by serial dilutions in PBS. The measurement protocol used to test the SPR-POF biosensor consisted of an initial conditioning step with viral culture medium (DMEM) diluted 1:100 in PBS. Then, samples containing viruses at increasing concentrations were dropped (50 µL volume) onto the sensitive surface of the biosensor and left to incubate for 10 min at room temperature, to ensure interaction between the target analyte and the bioreceptor. Subsequently, washing steps with PBS were performed to remove any non-specific binding, and then the transmitted spectra were recorded with PBS (blank) as bulk. The SPR spectra were obtained by normalizing the transmitted spectra acquired in PBS as bulk to the one acquired in air, considered as reference spectrum (since the SPR condition is not satisfied in air)[23]. Two NP swab samples, one negative and one positive to RSV, were stored in UTM and successively diluted in PBS before testing them. More specifically, the negative sample was diluted 1:100, while the positive one was diluted 1:100 and 1:50.

Ethical statement

The study was conducted in compliance with the Declaration of Helsinki. The protocol was approved by the Ethical Committee of the University Federico II of Naples (prot. no. 140/20). Informed consent was obtained from all individuals. At the time of sampling, laboratory parameters, clinical and demographic data were recorded.

Results and discussion

F protein Western blot analysis

In order to evaluate the binding capability of the anti-F ab used in the study, we assessed RSV protein F expression into our experimental setting. Cells were infected with RSV, harvested and lysed to obtain proteins at three different time points (6, 12 and 24 hpi). The expression level of F protein was analysed and normalised to GAPDH (Fig. 3, Figure S2 and Figure S3 in Supplementary Information File). It was observed that the protein amount was high at 24 hpi; therefore, these conditions were used in the following experiments.

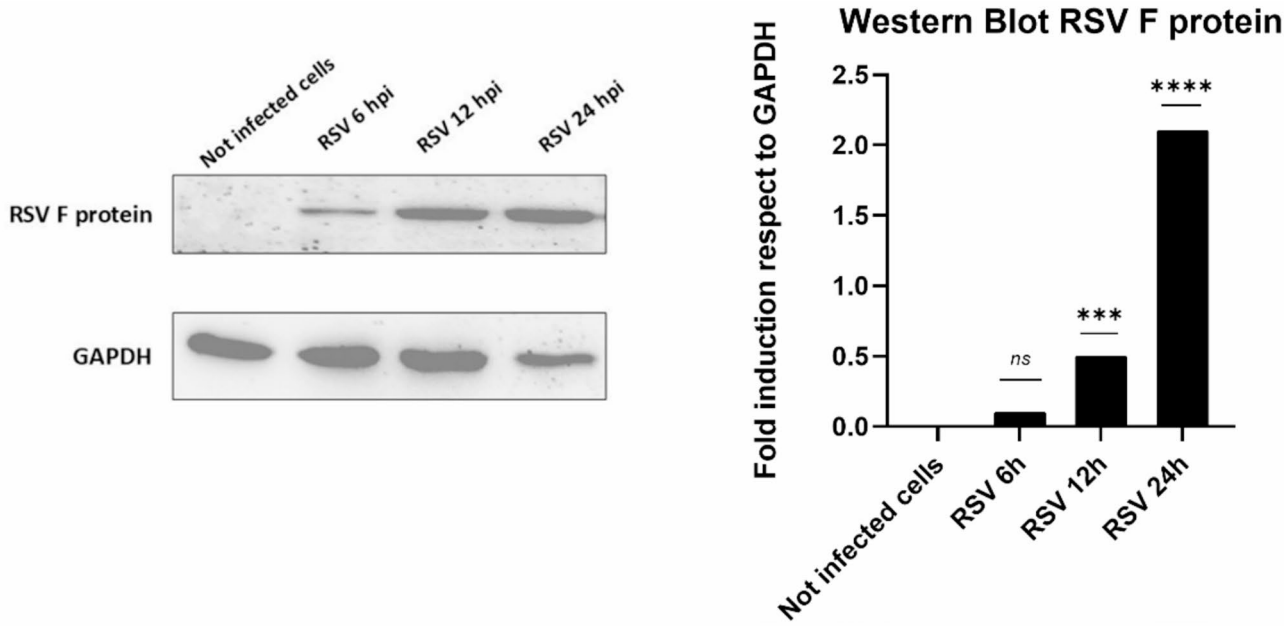

Fig. 3. Western-Blot. Cells were infected with RSV at MOI = 0.1; then, proteins were collected at three time points (6, 12 and 24 h). The expression of RSV F protein was high when infected cells were harvested after 24 h. Data are means of three independent experiments. ****$p < 0.0001$; **$p = 0.001$; ns = non-significant.

Dilution tested (PFU/mL)	Ct obtained in qPCR	
	Mean	SD
1	N/A	N/A
10	N/A	N/A
100	N/A	N/A
1000	21.76	0.44
10,000	16.84	0.15

Table 1. Amplification of F gene in RSV-infected cells at different dilutions. *Ct* threshold cycle, *n/a* not assigned.

qPCR results

qPCR is the most sensitive procedure able to detect very low viral titer. In order to set up our experimental scheme, cell monolayers were infected by using different RSV dilutions (in the range from 1 PFU/mL to 10000 PFU/mL). After 24 hpi, RNA was extracted using Trizol and reverse-transcribed into cDNA. Then, qPCR was executed in order to evaluate F gene expression. Results with a sigmoidal amplification curve and a cycle threshold (Ct) value ≤ 33 were considered positive, Ct-values between 34 and 40 inconclusive (N/A), and over Ct 40 were indicated as negative. Table 1 shows that amplification of RSV F gene was observed only at very high viral titers (1000 and 10000 PFU/mL), while data were inconclusive at lower dilutions. We also normalized Ct-values obtained for F gene respect to GAPDH (Figure S4 of the Supplementary Information File) observing a detectable protein expression only for the highest RSV dilutions.

RSV detection via SPR-POF biosensors

Binding tests in PBS

Following the functionalization process described in Materials and methods Section (see "Functionalization process of the SPR-POF probe" Section), SAM formation for RSV detection was verified by comparing SPR spectra acquired before and after the functionalization process, using PBS as the surrounding medium over the plasmonic sensing surface. The obtained SPR spectra are shown in Fig. 4.

In particular, as shown in Fig. 4, the functionalization caused a total resonance wavelength shift toward higher values (red-shift) of about 18 nm. This shift is a consequence of the increment of the RI at the interface between the nanometric gold surface and the dielectric medium due to the immobilization of the antibody SAM over the plasmonic surface. In other words, the resonance wavelength shift of 18 nm was achieved between the bare surface (gold surface without receptor layer) and the end of the functionalization process (via lipoic acid, NHS/EDC mixture, antibody, and ethanolamine), both considering the same solution (i.e., PBS) as the

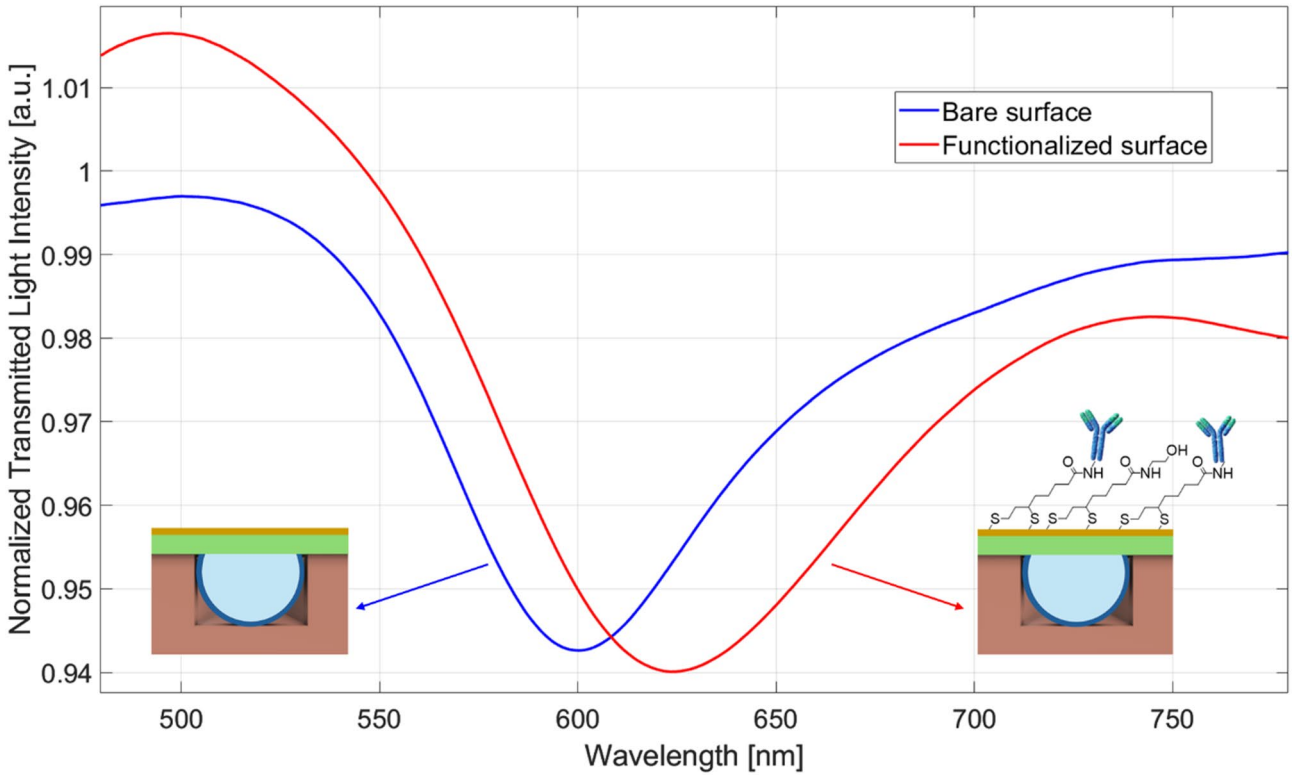

Fig. 4. SPR spectra acquired before (blue) and after (red) the SPR-POF probe functionalization process by considering the same bulk solution (PBS).

surrounding medium (i.e., bulk solution) deposited onto the sensitive surface. It should be noted that this variation in resonance wavelength following the functionalization procedure results in line with other SPR-POF biosensor configurations functionalized with a similar procedure but other bio-receptors[29,30].

Next, to determine the biosensor response to RSV, experimental tests were performed by challenging the sensitive surface with RSV diluted in PBS at different concentrations ranging from 0.1 to 10^4 PFU/mL.

The SPR spectra achieved by testing the developed SPR-POF biosensor with different concentrations of RSV in PBS solution are shown in Fig. 5a. More specifically, the resonance wavelength shifts toward lower values (blue-shift) as the virus concentration increases. This SPR shift indicates that, when binding between RSV and the bio-receptor layer occurs, the RI of the receptor layer in contact with the plasmonic surface decreases, similar to what was obtained in[24,25].

The experimental data were fitted by using the Langmuir model, obtained by considering $n = 1$ in the Hill equation reported in Eq. (1), attaining the dose-response curve shown in Fig. 5b.

In particular, the absolute value of the resonance wavelength variation ($|\Delta\lambda|$) calculated in respect to the blank (PBS solution without RSV), is reported in Fig. 5b as a function of the analyte concentration (c). The error bars (about 0.2 nm), calculated as the maximum standard deviation measured in tests with three similar biosensors, are shown in Fig. 5b, too.

The Hill model used in Fig. 5b by considering $n = 1$ is recalled following:

$$|\Delta\lambda_c| = |\lambda_c - \lambda_0| = |\Delta\lambda_{max}| \cdot \left(\frac{c^n}{K^n + c^n}\right). \quad (1)$$

where c is the analyte concentration, λ_c is the resonance wavelength at the concentration c, λ_0 is the resonance wavelength at zero concentration of RSV (blank solution), $\Delta\lambda_{max}$ is the maximum value of λ_c obtained at the signal saturation value, n and K are Hill fitting constants. In particular, when $n = 1$, as considered in this work, the Hill model coincides with the Langmuir one.

Equation (1) can be considered as a linear model when c is much lower than K; in this case, the slope of the linear equation ($\Delta\lambda_{max}/K$) is defined as the sensitivity at low concentration ($S_{low-conc}$).

Specifically, the Langmuir fitting parameters are reported in Table S1 of the Supplementary Information File and were obtained by using OriginPro 9 software (Origin Lab. Corp., Northampton, MA, USA).

In Table 2, the biosensing performance parameters are reported, meaning $S_{low-conc}$ and the limit of detection (LOD), which is calculated as the ratio between 3 times the standard deviation of the blank (St. error of λ_0 in Table S1) and the $S_{low-conc}$.

Finally, to compare the developed RSV biosensor with other kinds of biosensors, Table 3 reports a comparative analysis, in terms of LOD, between several biosensor configurations based on different sensing techniques.

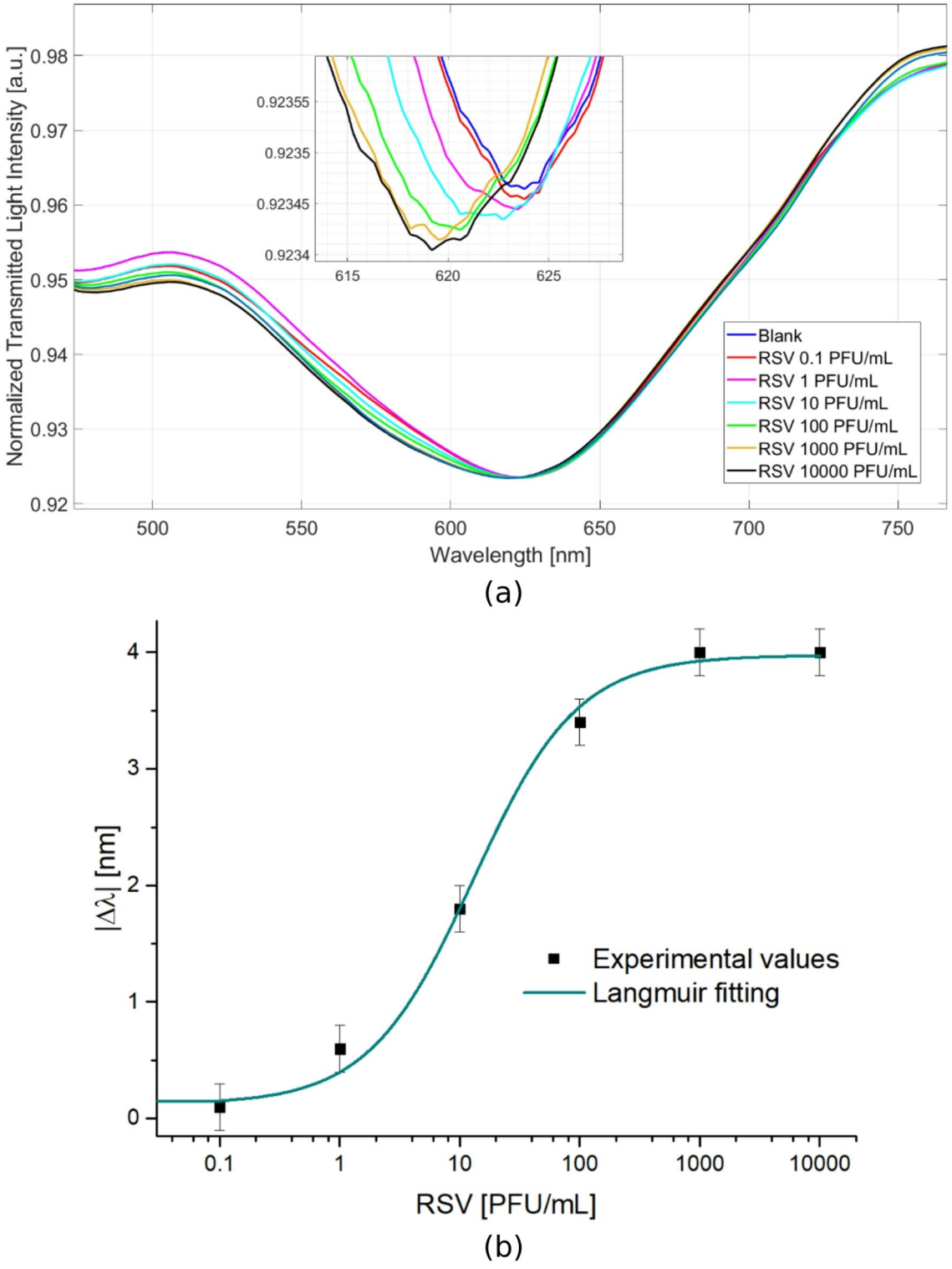

Fig. 5. (**a**) SPR spectra achieved by testing the SPR-POF biosensor with PBS solutions containing RSV at different concentrations (range 0.1–10^4 PFU/mL). (**b**) Dose-response curve of RSV detection in PBS. Absolute value of the resonance wavelength variation compared with the blank solution versus the virus concentrations on a semilogarithmic scale. The black squares represent the experimental values, and the dark cyan curve represents the fit of the experimental data using the Langmuir model. The error bar corresponds to the maximum standard deviation obtained by testing three biosensors under the same conditions.

LOD [PFU/mL]	$S_{low-conc}$ [nm ● mL/PFU]
0.88	0.31

Table 2. SPR-POF biosensor parameters for RSV detection in PBS.

Sensor configuration	Sensing method	LOD (PFU/mL)	References
Gold metallic nanoparticles conjugated to anti-RSV polyclonal antibody	Localized Surface Plasmon Resonance (LSPR)	211	[31]
Immunosensors based on screen-printed gold and glassy carbon (GC) disc electrodes	electrochemical	1.1×10^3	[32]
Modified pencil graphite electrode (PGE) coupled with anti-RSV monoclonal antibody	impedimetric	22.54	[33]
SiO_2 coated silver nanorod array substrates	Surface-enhanced Raman scattering (SERS)	391	[34]
Modified POF-based probe coupled with anti-RSV antibody	SPR	0.88	This work

Table 3. Comparison in terms of LOD between several RSV biosensor configurations.

As shown in Table 3, the proposed SPR-POF biosensor, exploiting a low-cost, small-size, and simple-to-use setup, presents an ultra-low detection limit with respect to the other presented RSV biosensors. Moreover, the POF-based sensor probe costs a few euros, and the functionalization process is very simple to realize.

The high sensitivity of the proposed biosensor can be exploited for quantitative detection of RSV, which is useful for evaluating the efficacy of pharmaceutical treatments. In fact, thanks to the obtained LOD, it is possible to dilute a real matrix with high dilution ratios. This allows minimizing non-specific interactions between different components of a real sample and the sensor, improving the accuracy of the results.

Selectivity tests

To evaluate the specificity of the developed RSV biosensor, a selectivity test was carried out by testing it with two interfering viruses, i.e., HCOV-229E and INFLA-H1N1. These viruses were specifically selected because they are responsible for clinical symptoms that closely resemble those caused by RSV, making them particularly relevant for differential diagnosis. The results reported in Fig. 6 show that both interferents, tested on the SPR-POF biosensor at a concentration of 100 PFU/mL, produced no significant resonance wavelength shift with respect to the blank (0 nm and 0.1 nm, respectively), minor than the error bars.

In contrast, RSV considered at a concentration of 10 PFU/mL (10 times lower than that of the interfering substances) produced a significant resonance wavelength shift of approximately 1.7 nm (in absolute value), as shown in Fig. 6.

Tests in real samples

In order to determine the applicability of the proposed RSV biosensor in a real scenario, additional tests were performed with NP swab samples, prepared and diluted, as described in Materials and methods Section (see "Samples Preparation and measurement protocol for SPR-POF biosensors" Section).

More specifically, SPR spectra were acquired by analyzing and comparing an NP-negative sample and one that tested positive on the 23rd cycle of RT-PCR. In Fig. 7a, it is shown that the negative sample produced no significant resonance wavelength shift (within the error bar value of 0.2 nm) with respect to the blank, whereas the positive sample tested at two different dilutions produced significant shifts. More specifically, the RSV concentration in the positive NP swab sample can be calculated by the resonance wavelength shifts achieved at different dilution factors (1:100 and 1:50) and the dose/response curve reported in Fig. 5b, as shown in Fig. 7b. In particular, by considering Fig. 7b, each resonance wavelength shift (obtained with different NP swab sample dilutions) indicated on the y-axis by orange lines can be used to estimate the corresponding RSV concentration on the x-axis. In this frame, Table 4 reports the absolute value of resonance wavelength shifts ($|\Delta\lambda|$) obtained at different dilution factors and the corresponding RSV concentration attained by the dose/response curve. In particular, the RSV concentration in the NP swab sample can be estimated by multiplying the concentration reported in Table 4 with the related dilution factor, thus obtaining an RSV concentration equal to about 400 PFU/mL.

Conclusions

In this work, a POCT based on a plasmonic POF probe coupled with a specific antibody for the detection of RSV was developed and experimentally tested. The binding tests in PBS demonstrated a noteworthy LOD of about 1 PFU/mL, resulting in a lower result than other RSV biosensors in the literature. High specificity was also successfully assessed by challenging the RSV biosensor with interfering viruses (i.e., HCOV-229E and INFLA-H1N1). Furthermore, preliminary tests performed on two NP swab samples (negative and positive to RSV) paved the way for applying this biosensing strategy as a tool in clinical diagnostics, in the view of POCTs, without requiring any sample pre-treatment. More specifically, the proposed POCT can be used for direct detection without the need for any preliminary sample lysis, significantly reducing the assay time to 10 min (compared to the 2 h typically required by the gold standard) while maintaining high sensitivity, three orders of magnitude better than the gold standard. The proposed sensing approach offers a significant advantage for

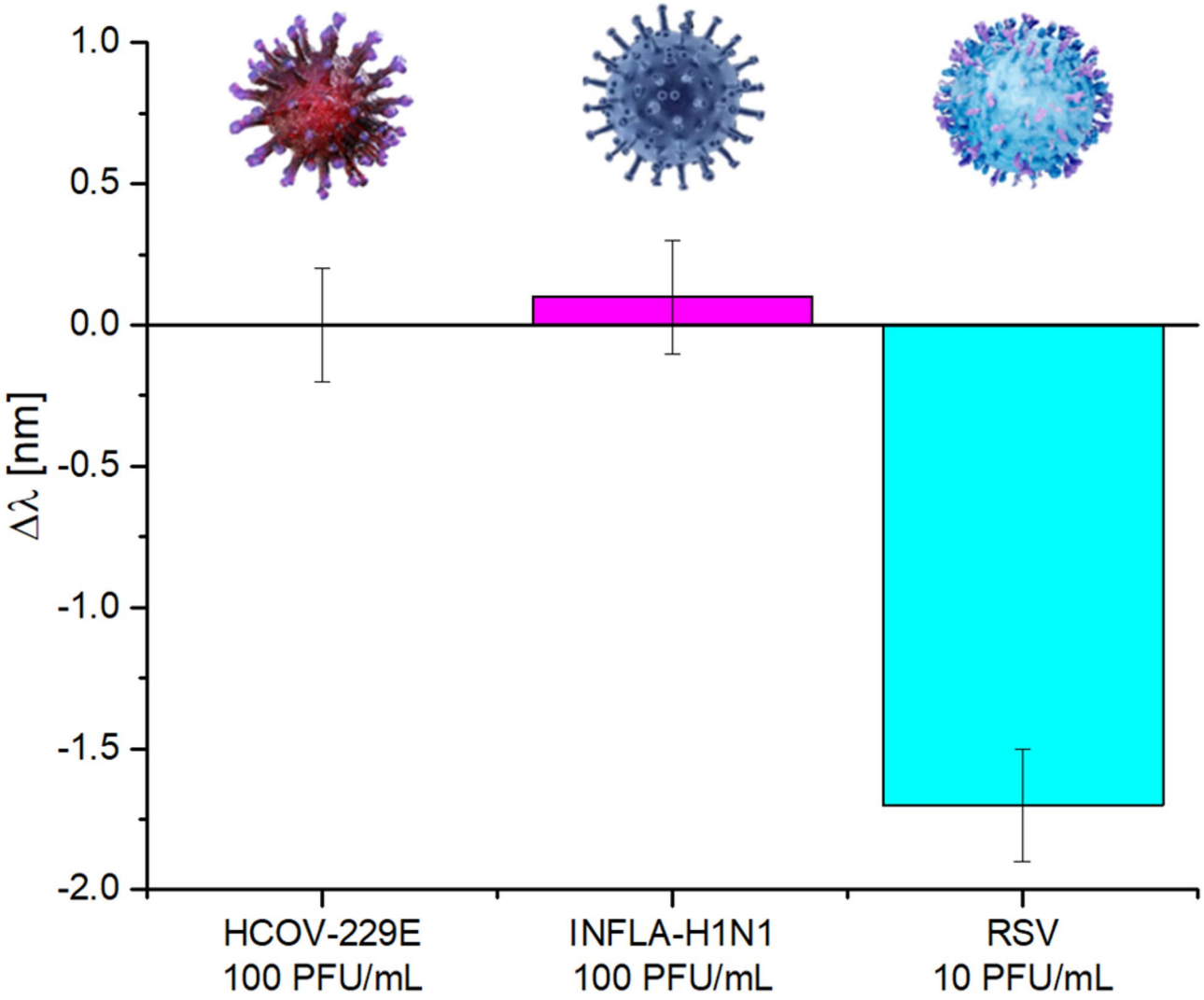

Fig. 6. Resonance wavelength variation (Δλ) obtained by testing the RSV biosensor with two interfering viruses HCOV-229E and INFLA-H1N1 (100 PFU/mL) and the target analyte (10 PFU/mL).

POCT implementation, as it simplifies the analytical procedure, shortens the overall assay time, and facilitates automation, even in low-resource settings or in the absence of highly specialized personnel.

This assay might add value in improving patient cohortation in emergency units and in primary health care units with long distances to a central laboratory, allowing a fast decision on patients' isolation or antiviral treatment. At variance with the POCTs now available due to the high sensitivity of this assay a confirmatory RT PCR test will not be required.

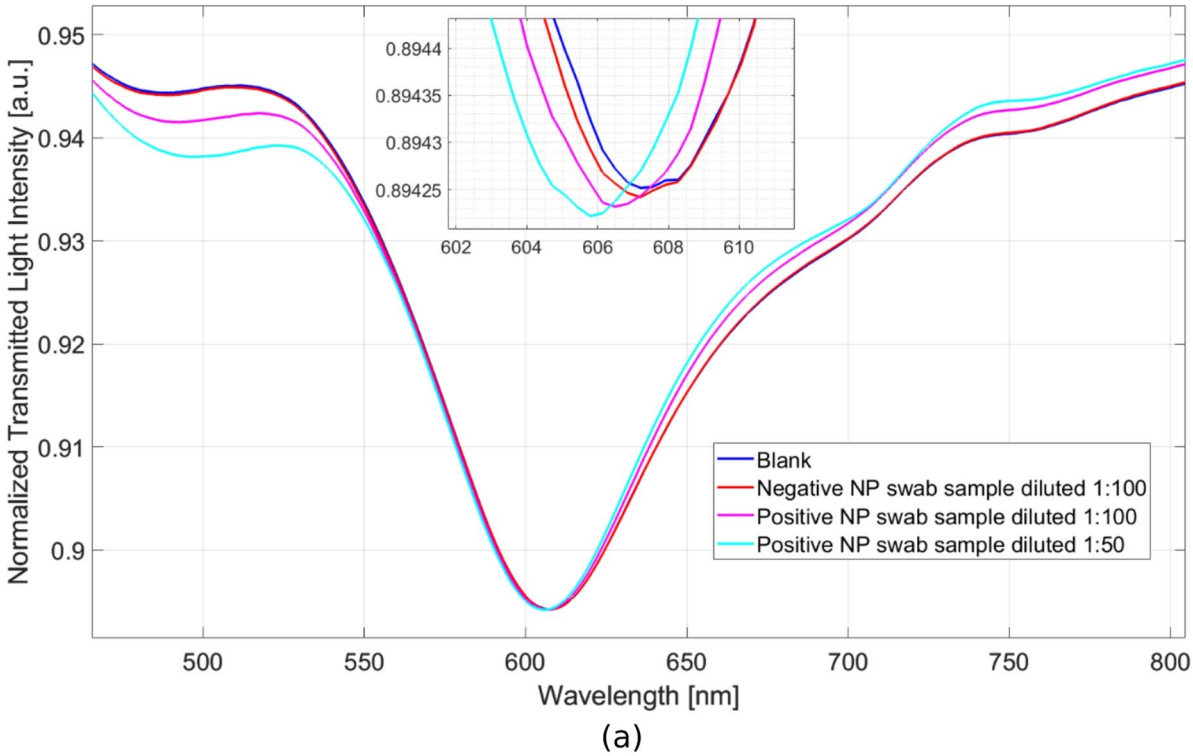

(a)

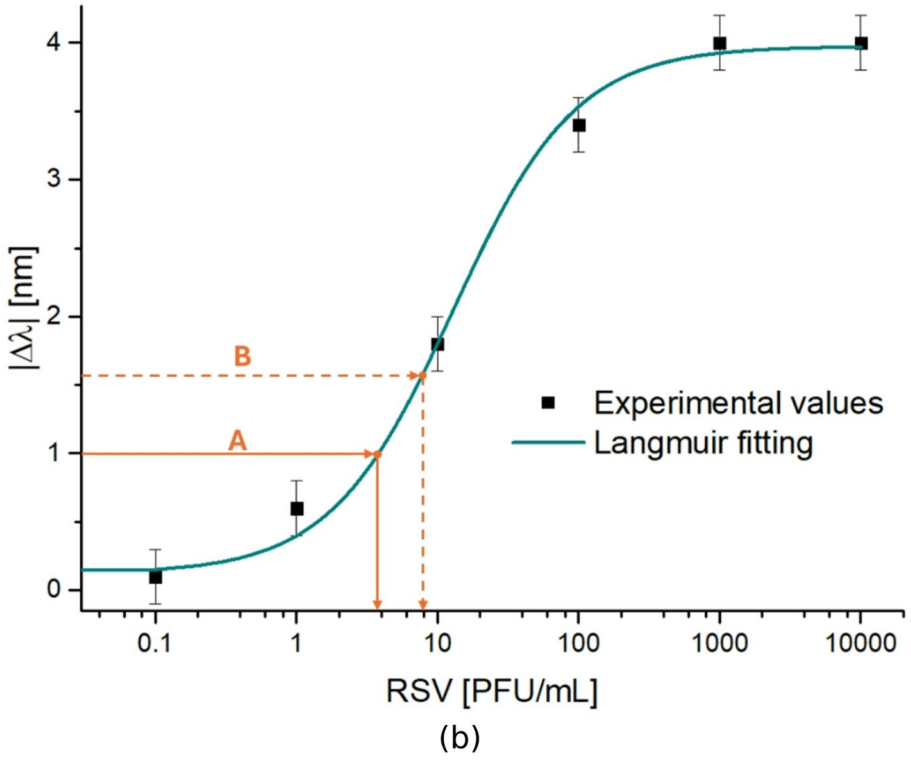

(b)

Fig. 7. (**a**) SPR spectra relative to RSV detection in two NP swab samples (negative and positive) diluted with PBS at different dilution factors (positive 23rd cycle of RT-PCR). (**b**) RSV concentration estimation in positive NP swab sample from the binding isotherm reported in Fig. 5b.

Label	Dilution factor	$\|\Delta\lambda\|$ [nm]	Estimated RSV concentration of the diluted positive NP swab sample [PFU/mL]	Estimated RSV concentration of the positive NP swab sample [PFU/mL]
A	1:100	1	3.9	3.9*100 = 390
B	1:50	1.6	8	8*50 = 400

Table 4. Summary of the SPR-POF biosensor response relative to the positive NP swab sample tested at different dilution factors and estimation of the RSV concentration from the binding isotherm.

Data availability

All data generated or analyzed during this study are included in this published article [and its supplementary information files], however raw data will be available from the corresponding author on reasonable request.The authors did not receive support from any organization for the submitted work.

Received: 16 January 2025; Accepted: 26 May 2025
Published online: 04 June 2025

References

1. Walsh, E.E. & Hall, C.B. Respiratory syncytial virus in Diagnostic procedures for viral and rickettsial infections (ed. Schmidt N.J., Emmons R.W.) 693–712 (American Public Health Association, 1989).
2. Wong, H., et al. The Molecular Epidemiology of Respiratory Syncytial Virus in Ontario, Canada from 2022–2024 using a Custom Whole Genome Sequencing Assay and Analytics Package.J. Clin. Virol., 176, 105759 (2024). https://doi.org/10.1016/j.jcv.2024.105759.
3. Anderson, L. et al. Strategic priorities for respiratory syncytial virus (RSV) vaccine development. *Vaccine* **31**, B209–B215. https://doi.org/10.1016/j.vaccine.2012.11.106 (2013).
4. Nuttens, C. et al. Differences between RSV A and RSV B subgroups and implications for pharmaceutical preventive measures. *Infect. Dis. Ther.* **13** (8), 1725–1742. https://doi.org/10.1007/s40121-024-01012-2 (2024).
5. Lambert, L., Sagfors, A. M., Openshaw, P. J. M. & Culley, F. J. Immunity to RSV in Early-Life. *Front. Immunol.* **5**, 466. https://doi.org/10.3389/fimmu.2014.00466 (2014).
6. Li, Y. et al. Global, regional, and National disease burden estimates of acute lower respiratory infections due to respiratory syncytial virus in children younger than 5 years in 2019: A systematic analysis. *Lancet* **399**, 2047–2064. https://doi.org/10.1016/S0140-6736(22)00478-0 (2022).
7. Terstappen, J. et al. The respiratory syncytial virus vaccine and monoclonal antibody landscape: the road to global access. *Lancet Infect. Dis.* **24**, e747–e761. https://doi.org/10.1016/s1473-3099(24)00455-9 (2024).
8. Chartrand, C., Tremblay, N., Renaud, C. & Papenburg, J. Diagnostic accuracy of rapid antigen detection tests for respiratory syncytial virus infection: systematic review and meta-analysis. *J. Clin. Microbiol.* **53** (12), 3738–3749. https://doi.org/10.1128/jcm.01816-15 (2015).
9. Bruning, A. H. L. et al. Rapid tests for influenza, respiratory syncytial virus, and other respiratory viruses: A systematic review and Meta-analysis. *Clin. Infect. Dis.* **65** (6), 1026–1032. https://doi.org/10.1093/cid/cix461 (2017).
10. Lu, S., Lin, S., Zhang, H., Liang, L. & Shen, S. Methods of respiratory virus detection: advances towards Point-of-Care for early intervention. *Micromachines* **12** (6), 697. https://doi.org/10.3390/mi12060697 (2021).
11. Zhang, Z. et al. Advanced Point-of-Care testing technologies for human acute respiratory virus detection. *Adv. Mater.* **34** (1). https://doi.org/10.1002/adma.202103646 (2021).
12. Savolainen, L. E. et al. Clinical performance of two commercially available rapid antigen tests for influenza, RSV, and SARS-CoV-2 diagnostics. *Microbiol. Spectr.* 13. https://doi.org/10.1128/spectrum.01630-24 (2024).
13. Gómez, S., Prieto, C., Vera, C., Otero, J. R. & Folgueira, L. Evaluation of a new rapid diagnostic test for the detection of influenza and RSV. Enferm. *Infecc Microbiol. Clin.* **34** (5), 298–302. https://doi.org/10.1016/j.eimc.2015.05.007 (2015).
14. Henrickson, K. J. & Hall, C. B. Diagnostic assays for respiratory syncytial virus disease. *J. Pediatr. Infect. Dis.* **26** (11), S36–S40. https://doi.org/10.1097/inf.0b013e318157da6f (2007).
15. Cennamo, N., Pesavento, M., Arcadio, F., Marzano, C. & Zeni, L. Advances in plastic optical fiber bio/chemical sensors to realize point-of-care-tests. *TrAC Trends Anal. Chem.* **177**, 117797. https://doi.org/10.1016/j.trac.2024.117797 (2024).
16. Pal, T., Aditya, S., Mathai, T. & Mukherji, S. Polyaniline coated plastic optic fiber biosensor for detection of aflatoxin B1 in nut, cereals, beverages, and body fluids. *Sens. Actuat B Chem.* **389**, 133897. https://doi.org/10.1016/j.snb.2023.133897 (2023).
17. Wu, X. et al. A D-Shaped polymer optical fiber surface plasmon resonance biosensor for breast cancer detection applications. *Biosensors* **14** (1), 15. https://doi.org/10.3390/bios14010015 (2023).
18. Wang, J., Xu, Z. & Kotsifaki, D. G. Plasmonic and metamaterial biosensors: a game-changer for virus detection. *Sens. Diagn.* **2** (3), 600–619. https://doi.org/10.1039/d2sd00217e (2023).
19. Kotsifaki, D. G., Singh, R. R., Chormaic, S. N. & Truong, V. G. Asymmetric split-ring plasmonic nanostructures for the optical sensing of Escherichia coli. *Biomed. Opt. Express*. **14** (9), 4875. https://doi.org/10.1364/boe.497820 (2023).
20. Cennamo, N. et al. Proof of concept for a quick and highly sensitive On-Site detection of SARS-COV-2 by plasmonic optical fibers and molecularly imprinted polymers. *Sensors* **21** (5), 1681. https://doi.org/10.3390/s21051681 (2021).
21. Cennamo, N. et al. SARS-CoV-2 Spike protein detection through a plasmonic D-shaped plastic optical fiber aptasensor. *Talanta* **233**, 122532. https://doi.org/10.1016/j.talanta.2021.122532 (2021).
22. Pasquardini, L. et al. Immuno-SPR biosensor for the detection of Brucella abortus. *Sci. Rep.* **13** (1). https://doi.org/10.1038/s41598-023-50344-5 (2023).
23. Cennamo, N., Massarotti, D., Conte, L. & Zeni, L. Low cost sensors based on SPR in a plastic optical fiber for biosensor implementation. *Sensors* **11** (12), 11752–11760. https://doi.org/10.3390/s111211752 (2011).
24. Guida, L. et al. An optical fiber-based point-of-care test for periodontal MMP-8 detection: A proof of concept. *J. Dent.* **134**, 104553. https://doi.org/10.1016/j.jdent.2023.104553 (2023).
25. Annunziata, M. et al. A novel plasmonic optical-fiber-based point-of-care test for periodontal MIP-1α detection. *iScience* **26** (12), 108539. https://doi.org/10.1016/j.isci.2023.108539 (2023).
26. Kõressaar, T. et al. Primer3_masker: integrating masking of template sequence with primer design software. *Bioinformatics* **34** (11), 1937–1938. https://doi.org/10.1093/bioinformatics/bty036 (2018).
27. Radhakrishnan, A. et al. Protein analysis of purified respiratory syncytial virus particles reveals an important role for heat shock protein 90 in virus particle assembly. *Mol. Cell. Proteom.* **9** (9), 1829–1848. https://doi.org/10.1074/mcp.M110.001651 (2010).

28. Chianese, A. et al. The antiherpetic and anti-inflammatory activity of the frog-derived peptide Hylin-a1. *J. Appl. Microbiol.* **135** (7), lxae165. https://doi.org/10.1093/jambio/lxae165 (2024).
29. Bencivenga, D. et al. Plasmonic optical fiber biosensor development for point-of-care detection of malondialdehyde as a biomarker of oxidative stress. *Free Radic Biol. Med.* **199**, 177–188. https://doi.org/10.1016/j.freeradbiomed.2023.02.020 (2023).
30. Cennamo, N. et al. Plasmon resonance biosensor for interleukin-1β point-of-care determination: A tool for early periodontitis diagnosis. *iScience* **27** (1), 108741. https://doi.org/10.1016/j.isci.2023.108741 (2023).
31. Valdez, J., Bawage, S., Gomez, I. & Singh, S. R. Facile and rapid detection of respiratory syncytial virus using metallic nanoparticles. *J. Nanobiotechnol.* **14** (1), 13. https://doi.org/10.1186/s12951-016-0167-z (2016).
32. Białobrzeska, W. et al. Electrochemical immunosensors based on Screen-Printed gold and glassy carbon electrodes: comparison of performance for respiratory syncytial virus detection. *Biosensors* **10** (11), 175. https://doi.org/10.3390/bios10110175 (2020).
33. Silva, T. S. E., Freitas, G. R. O. E., Ferreira, L. F. & Franco, D. L. Development of a label-free impedimetric immunosensor for the detection of respiratory syncytial virus. *J. Solid State Electrochem.* **28** (11), 4015–4027. https://doi.org/10.1007/s10008-024-05999-z (2024).
34. Yang, Y. et al. Rapid and quantitative detection of respiratory viruses using surface-enhanced Raman spectroscopy and machine learning. *Biosens. Bioelectron.* **217**, 114721. https://doi.org/10.1016/j.bios.2022.114721 (2022).

Acknowledgements

The authors N.C. and L.Z. acknowledge the support of the European Union by the Next Generation EU project PRIN2022 – 2022JRKETK – "BOHEMIAN" (Versatile hybrid in-fiBer Optical-electrocHemical systEMs for wIdely Applicable bioseNsing) and by the Next Generation EU project "BIOMULTIMETRO" (BIO-sensori per MULTI-analiti in METRiche Opportune).

Author contributions

F.P., F.A., G.P., L.Z. and N.C.: conceived and designed the experiments. F.P., F.A., G.P., L.Z., M.G., C.Z., A.D., C.M., I.T., F.N., R.P., and N.C.: Performed the experiments, analyzed the data, and prepared figures. F.P., F.A., G.P., C.Z. and N.C.: Wrote the paper. All authors reviewed and approved the final version of the manuscript.

Funding

The authors did not receive support from any organization for the submitted work.

Declarations

Competing interests

The authors declare no competing interests.

Additional information

Supplementary Information The online version contains supplementary material available at https://doi.org/10.1038/s41598-025-04239-2.

Correspondence and requests for materials should be addressed to G.P. or N.C.

Reprints and permissions information is available at www.nature.com/reprints.

Publisher's note Springer Nature remains neutral with regard to jurisdictional claims in published maps and institutional affiliations.